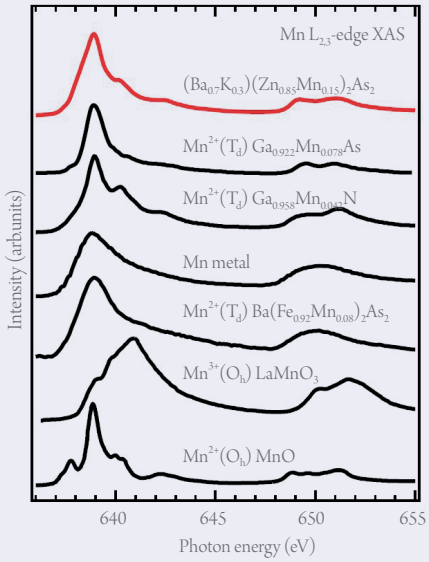

Fig. 2: Mn $L_{2,3}$-edge XAS of Mn-$BaZn_2As_2$, compared with those of $Ga_{0.922}Mn_{0.078}As$, $Ga_{0.958}Mn_{0.042}N$, Mn metal, $Ba(Fe_{0.92}Mn_{0.08})_2As_2$, $LaMnO_3$, and MnO. The valence and local symmetry of Mn atoms are indicated for each compound. [Reproduced from Ref. 6]

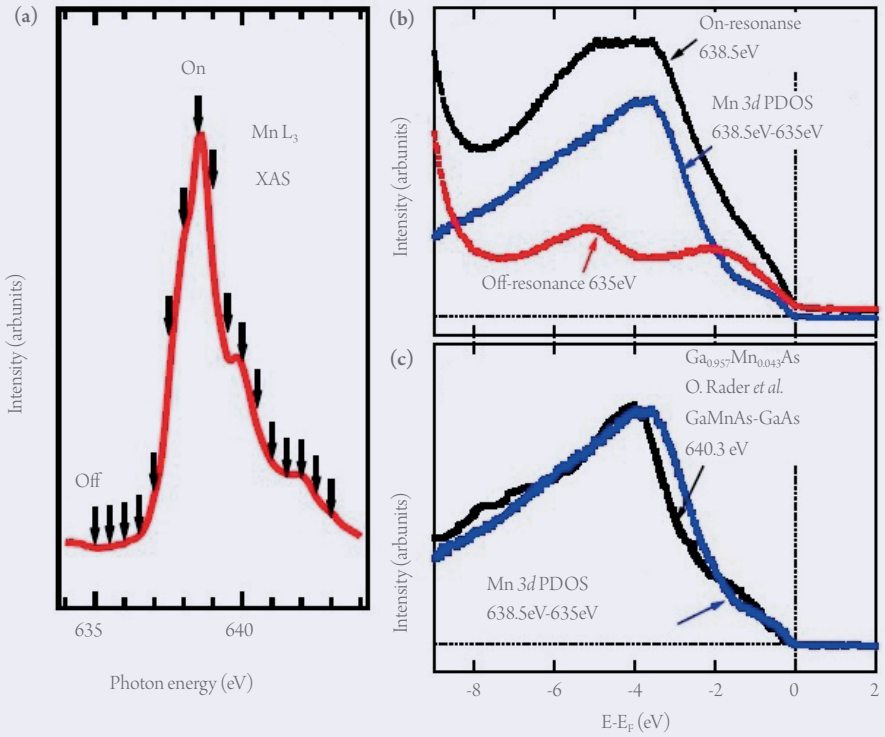

Fig. 3: (a) On- and off-resonance photon energies are shown with arrows on Mn L_3-edge XAS of Mn-$BaZn_2As_2$. (b) Mn 3*d* PDOS deduced on subtracting the off-resonance spectrum ($h\nu = 635$ eV) from the on-resonance spectrum ($h\nu = 638.5$ eV). (c) Mn 3*d* PDOS of $Ga_{0.957}Mn_{0.043}As$ (Ref. 7) compared with that of Mn-$BaZn_2As_2$. [Reproduced from Ref. 6]

Suzuki *et al.* studied the electronic structures of $Ba_{1-x}K_x(Zn_{1-y}Mn_y)_2As_2$ related to Mn 3*d* states using XAS and RPES measurements. The Mn $L_{2,3}$-edge XAS indicate that the doped Mn atoms have a valence 2+ and are strongly hybridized with the As 4*p* orbitals, as in archetypical DMS GaMnAs. The Mn 3*d* PDOS obtained from RPES leads to the d^5 electronic configurations of Mn atoms with local magnetic moment $S = 5/2$. They concluded that the doped holes go into the top of the As 4*p*-derived valence band and are weakly bound to the Mn local spins. The ferromagnetic correlation between the local spins mediated by the hole carriers induces ferromagnetism in Mn-$BaZn_2As_2$. (Reported by Jun Okamoto)

This report features the work of Hakuto Suzuki, Atsushi Fujimori and their co-workers published in Phys. Rev. B ***95****, 140401(R) (2015).*

References

1. H. Ohno, Science **281**, 951 (1998).
2. T. Dietl, Nature Mater. **9**, 965 (2010).
3. K. Zhao, Z. Deng, X. C. Wang, W. Han, J. L. Zhu, X. Li, Q. Q. Liu, R. C. Yu, T. Goko, B. Frandsen, L. Liu, F. Ning, Y. J. Uemura, H. Dabkowska, G. M. Luke, H. Luetkens, E. Morenzoni, S. R. Dunsiger, A. Senyshyn, P. Bni, and C. Q. Jin, Nature Commun. **4**, 1442 (2013).
4. M. Rotter, M. Tegel, and D. Johrendt, Phys. Rev. Lett. **101**, 107006 (2008).
5. K. Zhao, B. Chen, G. Zhao, Z. Yuan, Q. Liu, Z. Deng, J. Zhu, and C. Jin, Chin. Sci. Bull. **59**, 2524 (2014).
6. H. Suzuki, K. Zhao, G. Shibata, Y. Takahashi, S. Sakamoto, K. Yoshimatsu, B. J. Chen, H. Kumigashira, F.-H. Chang, H.-J. Lin, D. J. Huang, C. T. Chen, B. Gu, S. Maekawa, Y. J. Uemura, C. Q. Jin, and A. Fujimori, Phys. Rev. B **91**, 140401(R) (2015).
7. O. Rader, C. Pampuch, A. M. Shikin, W. Gudat, J. Okabayashi, T. Mizokawa, A. Fujimori, T. Hayashi, M. Tanaka, A. Tanaka, and A. Kimura, Phys. Rev. B **69**, 075202 (2004).

New Features of Topological Insulators from Terahertz Emission Spectroscopy

Topological insulators (TI) are a fascinating form of quantum matter that possesses a Dirac cone-like conducting surface state on its surfaces. The surface state exhibits novel properties, such as time-reversal protection against back- scattering and spin-polarized current. TI were predicted to have a high potential in applications of quantum computation. From the point of view of experimental study of TI, two key issues are how to determine the surface state and what characteristic properties the Dirac fermions possess. Several experimental techniques, such as angle-resolved photoemission spectroscopy (ARPES) and scanning tunneling microscopy, have been applied to gain insights on these issues.

For example, an unoccupied second surface state (second SS) and bulk bands (BB) located above the first SS by 1.5 eV have been observed in Bi_2Se_3 with the two-photon photoemission spectroscopy of ARPES measurements.[1] These second SS and BB play important roles in TI's optical coupling and related optoelectronic applications. Earlier studies on TI with optical spectroscopy, such as second harmonic generation and pump-probe measurements,[2,3] did not clearly identify the influences of these second SS and BB. This is because, during the optical excitation there are numerous phenomena occur simultaneously, such as photo-electron emission, nonlinear light conversion and generation of hot photo-carriers. Recently, it was proposed that terahertz (THz) emission was suggested to be a potential candidate capable of examining not only nonlinear light conversion but also transient dynamics of photo-excited carriers. In the THz and mid-infrared spectral ranges, electric-field-resolved light is a practical approach, which yields abundant information from the materials because of the available phase information of the light.

Chien-Ming Tu and his co-workers measured the THz emission spectra of TI samples with varied doping.[4] Figure 1(a) shows the schematics of their experiments. P-polarized 75-fs optical pump pulses, at wavelength 800 nm, illuminated the (111) surfaces of TI crystals at incident angle 45° to generate THz radiation; the emitted THz waveform

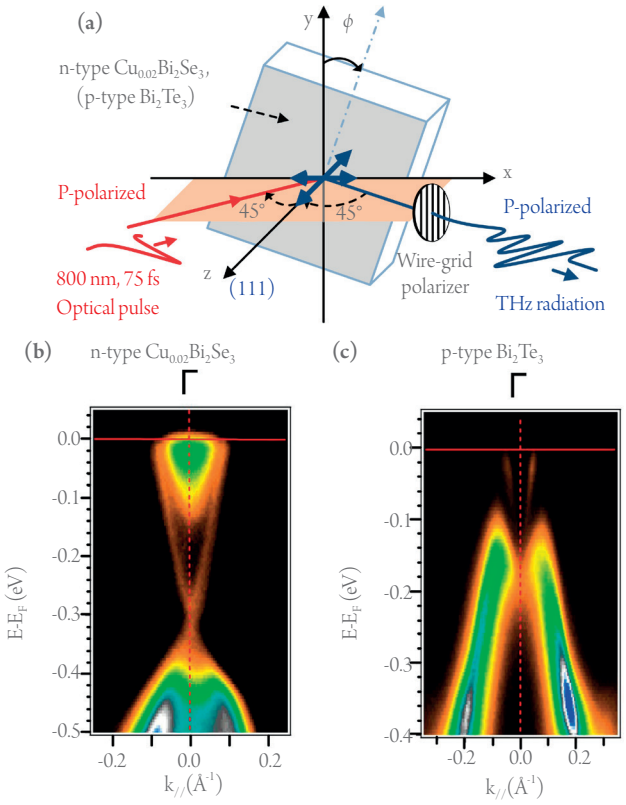

Fig. 1: (a) Schematic for THz emission from TI. P-polarized optical pulses irradiated the (111) surface of TI, and P-polarized THz radiation was detected after a wire-grid polarizer. The thick arrows denote in-plane and out-of-plane electric fields. (b)-(c) ARPES images of *n*-type $Cu_{0.02}Bi_2Se_3$ and p-type Bi_2Te_3. [Reproduced from Ref. 4]

was measured with electro-optic sampling. A wire-grid polarizer was set to detect P-polarized THz radiation. Figures 1(b) and 1(c) show the APRES images of the used samples. Two doped samples, *n*-type $Cu_{0.02}Bi_2Se_3$ (energy band gap ~0.3 eV) and *p*-type Bi_2Te_3 (energy band gap ~0.15 eV), were used in this work. The ARPES images were recorded at **BL21B1**.

Figures 2(a) and 2(b) show the measured few-cycle THz pulses from variously doped samples. In Figs. 2(c) and 2(d), comparison with X-ray diffraction results and THz amplitude ϕ-scan results shows no three-fold symmetry in a THz amplitude ϕ-scan. The directions of the P-polarized THz pulses are hence parallel to the surface normal of the samples; the P-polarized THz pulses are the results of the transient photocurrent induced by optical pulses. Interestingly, Tu *et al.* observed a polarity reversal as the samples switched from n-type to p-type, as shown in Figs. 2(a) and 2(b). The directions of the transient photo-excited current are hence anti-parallel near the surfaces. This phenomenon is entirely different from that observed in common narrow-band-gap semiconductors, such as InAs (energy band gap ~0.36 eV) and InSb (energy band gap ~0.17 eV); the diffusion current picture in InAs (InSb) cannot explain the polarity reversal of THz emission from TI with varied doping.

The recently discovered second SS and BB can elegantly resolve the paradox, as shown in Fig. 2(e). Because of the wide effective band gap (~1.5 eV) between the second SS and the first SS, the effective band gap matches the photon energy (1.55 eV at 800 nm) of the optical pump pulse, which provides extra energy loss for the photo-excited carriers. Surface field $E_{surface}$ due to band bending causes drift current J_{drift} and results in a polarity reversal of the THz pulse emitted from *p*-type Bi_2Te_3.

Tu's work shows not only the band structure of TI is important on optical coupling but also the potentials of time-domain THz emission spectroscopy. Tu's findings also expose some interesting issues for for future stueis, such as the dependence on photon energy and circular dichroism. This work shows also the uniquenessof bringing laser-based and synchrotron-based spectroscopy together. (Reported by Cheng-Maw Cheng)

This report features the work of Chien-Ming Tu, Chih-Wei Luo, Cheng-Maw Cheng and their co-workers published in Sci. Rep. ***5****, 14128 (2015).*

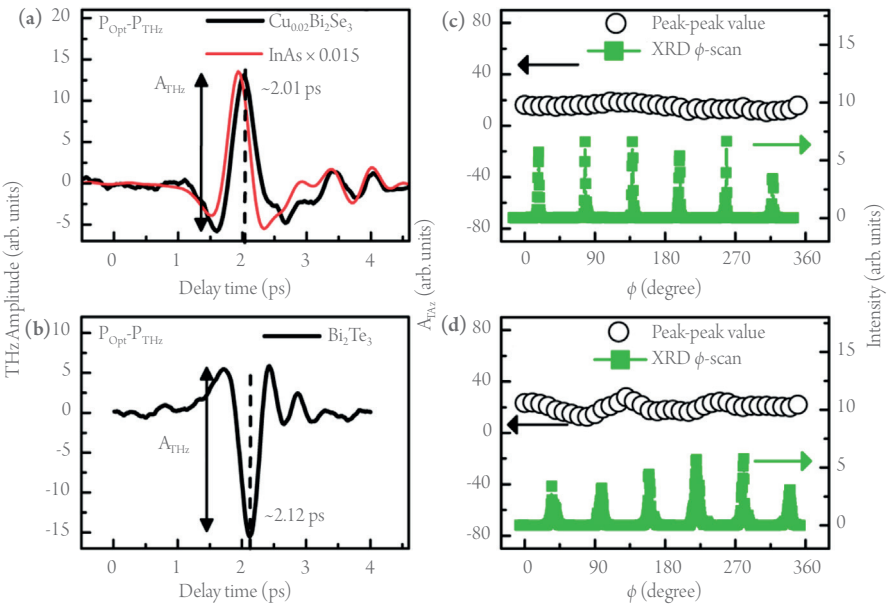

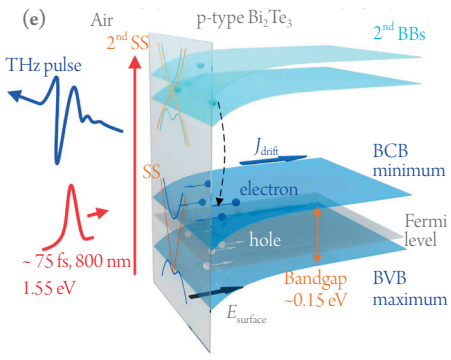

Fig. 2: (a)-(b) P-polarized THz waveform emission from *n*-type $Cu_{0.02}Bi_2Se_3$ and *p*-type Bi_2Te_3 after P-polarized optical-pulse excitation. In (a), the thin red line represents the 0.015-times smaller P-polarized THz wave generated from *n*-type InAs under the same conditions. The polarity of the THz waveform from *p*-type Bi_2Te_3 is reversed from that of *n*-type $Cu_{0.02}Bi_2Se_3$. (c)-(d): Plots of amplitude peak to peak as a function of azimuthal angle (ϕ-scan) of TI. The corresponding X-ray diffraction ϕ-scans for the (1 1 15) line for both single crystals are also shown (green). (e) Schematic for the influence of the second SS and BB on P-polarized THz emission from *p*-type Bi_2Te_3. BCB: bulk conduction band. BVB: bulk valence band. The second SS and BB would be responsible for the energy loss of the photo-excited carriers. Surface field $E_{surface}$ induced by band bending thus results also in drift current J_{drift} in the narrow-band-gap materials. [Reproduced from Ref. 4]

References

1. J. A. Sobota, S.-L. Yang, A. F. Kemper, J. J. Lee, F. T. Schmitt, W. Li, R. G. Moore, J. G. Analytis, I. R. Fisher, P. S. Kirchmann, T. P. Devereaux, and Z.-X. Shen, Phys. Rev. Lett. **111**, 136802 (2013).
2. D. Hsieh, F. Mahmood, J. W. McIver, D. R. Gardner, Y. S. Lee, and N. Gedik, Phys. Rev. Lett. **107**, 077401 (2011).
3. N. Kumar, B. A. Ruzicka, N. P. Butch, P. Syers, K. Kirshenbaum, J. Paglione, and H. Zhao, Phys. Rev. B **83**, 235306 (2011).
4. C.-M. Tu, T.-T. Yeh, W.-Y. Tzeng, H.-J. Chen, S.-A. Ku, C.-W. Luo, J.-Y. Lin, K.-H. Wu, J.-Y. Juang, T. Kobayashi, C.-M. Cheng, K.-D. Tsuei, H. Berger, R. Sankar, and F.-C. Chou, Sci. Rep. **5**, 14128 (2015).